Johann Radon Institute for
Computational and Applied Mathematics
Austrian Academy of Sciences (ÖAW)

Early Afterdepolarizations with Growing Amplitudes do not Require Stable Limit Cycles in the Fast Subsystem of Cardiac Action Potential Models

P. Kuegler

RICAM-Report 2015-17

Noname manuscript No.
(will be inserted by the editor)

Early Afterdepolarizations with Growing Amplitudes do not Require Stable Limit Cycles in the Fast Subsystem of Cardiac Action Potential Models

Philipp Kügler

Received: date / Accepted: date

Abstract Early afterdepolarizations (EADs) are pathological oscillations in cardiac action potentials during the repolarization phase and may be caused by drug side effects, ion channel disease or oxidative stress. The most widely observed EAD pattern is characterized by oscillations with growing amplitudes. So far, its occurence is explained in terms of a supercritical Hopf bifurcation in the fast subsystem of the action potential dynamics from which stable limit cycles with growing amplitudes emerge. In this article we demonstrate that EAD patterns with growing amplitudes do not require supercritical Hopf bifurcations in the fast subsystem but can also arise from loss of stability at subcritical Hopf or limit point bifurcations.

Keywords cardiac action potential · early afterdepolarization · dynamical system · bifurcation analysis · multiple time scales

1 Introduction

The term action potential (AP) refers to the characteristic membrane voltage response of excitable cells such as cardiomyocytes to a superthreshold elec-

P. Kügler
Institute of Applied Mathematics and Statistics, University of Hohenheim
Schloss 1
70599 Stuttgart, Germany
Tel.: +49-711-459-22388
Fax: +49-711-459-23030
E-mail: philipp.kuegler@uni-hohenheim.de
and
Mathematical Methods in Molecular and Systems Biology
Radon Institute for Computational and Applied Mathematics
Apostelgasse 23
1030 Vienna, Austria
Tel.: +43-1-51581-6551
E-mail: philipp.kuegler@oeaw.ac.at

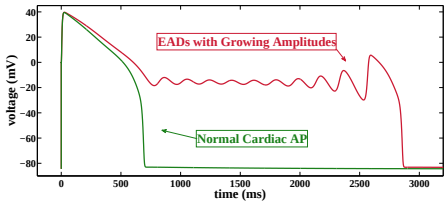

Fig. 1 Green curve shows simulation of cardiac action potential with depolarization due to superthreshold stimulation and normal repolarization back to resting potential. Red curve shows an AP distorted by early afterdepolarizations with growing amplitudes.

tric stimulus, see Figure 1. Cardiac APs are regulated by a subtle interplay of various ion channels [4] that control the in- and outflow of ions across the membrane. If this interplay is perturbed by pharmaceutical compounds [2], oxidative stress [20] or cardiac disease [11], the AP gets impaired and early afterdepolarizations (EADs) may arise. EADs are pathological voltage oscillations during the AP repolarization (or plateau) phase, see Figure 1, that may synchronize and trigger potentially lethal ventricular fibrillation [16].

At the cellular level, cardiac APs are modelled by means of coupled systems of nonlinear ODEs that consider the cellular membrane as an electrical circuit consisting of a capacitative current in parallel with several transmembrane ionic currents. Therein, the voltage equation

$$C\frac{dV}{dt} = -\sum_{ion} I_{ion}$$

is complemented by additional ODEs for channel gating variables that describe the voltage dependent activation and deactivation of the ionic currents. Modern cardiac AP models for animal [5], human adult [12] and human induced pluripotent stem cell derived [13] cardiomyocytes comprise dozens of state variables and hundreds of model parameters.

Using AP models of lower dimension, cardiac arrhythmias have been associated with bifurcations [3], [6] in the nonlinear AP dynamics. In particular, the on- and offset of EADs have been linked in [18], [14] with supercritical Hopf and saddle-homoclinic bifurcations in the fast subsystem of a four dimensional AP model, see Section 2 for details. This bifurcation scenario features stable limit cycles with growing amplitudes and currently is considered [17] to be necessary for the occurence of EADs with growing amplitudes (which is the most widely observed EAD pattern in experiments).

In this paper we demonstrate that stable limit cycles in the fast subsystem of cardiac AP models are not the only possible explanation for EAD patterns with growing amplitudes. In particular we illustrate that this EAD pattern may also result from loss of stability at subcritical Hopf or limit point bifur-

cations in the fast subsystem - two scenerios that do not involve stable limit cycles. The paper is organized as follows. Section 2 reviews the current bifurcation hypothesis on EAD genesis advertized in [18], [14], [3], [6], [17] but as a novelty leads the discussion from the perspective of delayed Hopf bifurcations in dynamical systems with multiple time scales [7]. Then, Section 3 illustrates how EAD dynamics with growing amplitudes alternatively may occur via a passage of the solution curve through a subcritical Hopf bifurcation in the fast subsystem. Furthermore, Section 4 demonstrates that this EAD pattern may also arise in a Hopf-free setting when the solution curve approaches a saddle-focus fixed point of the full AP system that coincides with a limit point bifurcation of the fast subsystem. After shortly commenting on EAD patterns with decreasing amplitudes in section 5, we finally show in section 6 that our findings are not model-specific and point to future directions of research.

2 EADs with Growing Amplitudes via Stable Limit Cycles in the AP Fast Subsystem

The current bifurcation hypothesis on the generation of EADs with growing amplitudes featured in [14], [3], [6], [17] was introduced in [18]. Therein, the authors used the AP model

$$\begin{aligned} C\frac{dV}{dt} &= -G_{Ca}df(V-E_{Ca}) - G_K x\bar{x}(V)(V-E_K) - I_0(V), \\ \frac{dd}{dt} &= \frac{d_\infty(V)-d}{\tau_d(V)}, \\ \frac{df}{dt} &= \frac{f_\infty(V)-f}{\tau_f(V)}, \\ \frac{dx}{dt} &= \frac{x_\infty(V)-x}{\tau_x(V)}, \end{aligned} \tag{1}$$

which is a reduced version of the Luo-Rudy model [10] for mammalian ventricular cells. This model includes the inward calcium current

$$I_{Ca} = G_{Ca}df(V-E_{Ca})$$

with the calcium channel conductance G_{Ca} and the dynamic activation and inactivation variables d and f as well as the outward potassium current

$$I_K = G_K x\bar{x}(V)(V-E_K)$$

with the potassium channel conductance G_K and the dynamic activation variable x. The voltage dependent functions of the model include the inactivation variable $\bar{x}$, the background current I_0 as well as the relaxation variables τ_d, τ_f, τ_x and the steady states d_∞, f_∞, x_∞ of channel gating.

For biophysical reasons one may argue that the activation of the potassium current is a much slower process than the activation and deactivation of the

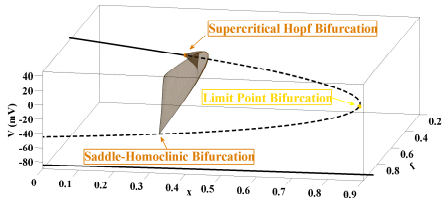

Fig. 2 Bifurcation diagram for the fast subsystem (2) with x as continuation parameter. Black solid and dashed curves represent stable and unstable fixed points of (2). At the supercritical Hopf bifurcation the stable focus-nodes turn into unstable fixed points of the saddle-focus type. Furthermore, a branch of stable limit cycles arises which terminates at a saddle-homoclinic bifurcation. At the limit point bifurcation the saddle-focus branch collides with a branch of unstable fixed points of the saddle type. The lower branch of fixed points is formed by stable nodes.

calcium current [4]. This motivates the consideration of (1) as a $(3,1)$ fast-slow system with the fast variables V, d, f and the slow variable x. Then, the associated fast subsystem is given by

$$\begin{aligned} C\frac{dV}{dt} &= -G_{Ca}df(V-E_{Ca}) - G_K x\bar{x}(V)(V-E_K) - I_0(V), \\ \frac{dd}{dt} &= \frac{d_\infty(V)-d}{\tau_d(V)}, \\ \frac{df}{dt} &= \frac{f_\infty(V)-f}{\tau_f(V)}. \end{aligned} \tag{2}$$

The bifurcation analysis [18] of (2) with x as continuation parameter reveals that (2) may possess a supercritical Hopf bifurcation at the upper branch of fixed points, see Figure 2 for the bifurcation diagram obtained with the model parameter values from [18]. From that Hopf point a branch of stable limit cycles emerges that subsequently terminates at a saddle-homoclinic bifurcation, i.e., at an orbit that is homoclinic to one of the saddle points along the middle branch of fixed points.

The bifurcation scenario illustrated in Figure 2 was used in [18] to explain the generation of EADs with growing amplitudes as follows. If the trajectory of the full system (1) is driven into the basin of attraction of the the branch of stable focus-nodes of the fast subsystem (2), a spiral movement is triggered. As the solution curve of (1) progresses along the branch of fixed point towards the supercritical Hopf bifurcation, the amplitudes decrease due to the negative real part of the complex eigenvalues. After the Hopf bifurcation the oscillations start to grow as the trajectory of (1) is attracted towards the stable limit cycles of (2) until the latter are terminated at the saddle-homoclinic bifurcation. Figure 3 illustrates this EAD generating mechanism by a projection of the solution curves of Figure 1 onto the (x, f, V)-space. If the trajectory passes by the basin of attractions of the fast subsystem (2), no EADs occur such that a normal action potential is generated. The difference between the two

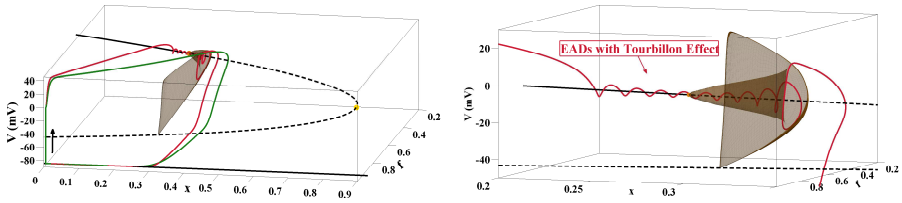

Fig. 3 Projection of two trajectories of the full system (1) onto the (x,f,V)-space. If the solution curve of (1) passes by the basins of attraction of the fast subsystem, no EADs occur. EADs with growing amplitudes are generated if the trajectory passes through the supercritical Hopf point of (2) before being pulled towards stable limit cycles with increasing amplitudes. From the perspective of a delayed Hopf bifurcation the situation shown corresponds to the Tourbillon effect.

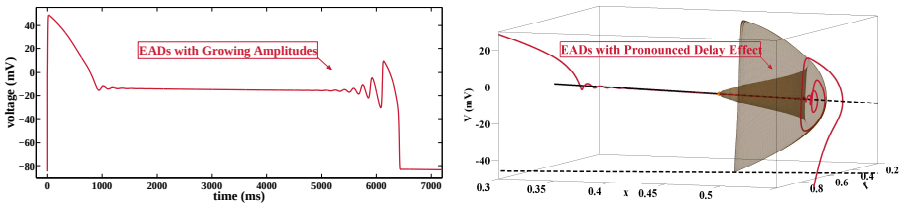

Fig. 4 Generation of EADs with growing amplitudes by passage through a supercritical Hopf bifurcation with pronounced delay effect. In vicinity of the Hopf point the oscillations are too small to be observed, only in some distance from the Hopf point the trajectory starts to follow the branch of stable limit cycles of the fast subsystem before their extinction at the saddle-homoclinic bifurcation.

solution curves results is due to different speeds of the x-activation (realized by different parameter settings in the x-equation of (1)) which, however, does not impact the fast subsystem (2) and hence the location of its fixed points and bifurcation points.

In the theory of multiple time scale dynamics [7], a Hopf bifurcation in a fast subsystem of a fast-slow system in which a slow variable acts as Hopf bifurcation parameter is called a delayed Hopf bifurcation. The term delay accomodates the fact that the solution curve of the full system remains close to the repelling branch of unstable fixed points for a substantial time after the Hopf bifurcation. From that perspective the scenario presented in [18] and illustrated in Figure 3 can be considered as a Tourbillon effect since the small scale oscillations in vicinity of the Hopf point are visible.

Next, we introduce two additional types of EAD generation with growing amplitudes than can be associated with the bifurcation constellation displayed in Figure 2. First, Figure 4 illustrates the scenario in which the trajectory of (1) still passes through the supercritical Hopf point but now undergoes a much more pronounced delay effect - in vicinity of the supercritical Hopf bifurcation the oscillations are too small to be visible. Only in some distance from the Hopf point the oscillations become visible again due to a jump into the basin

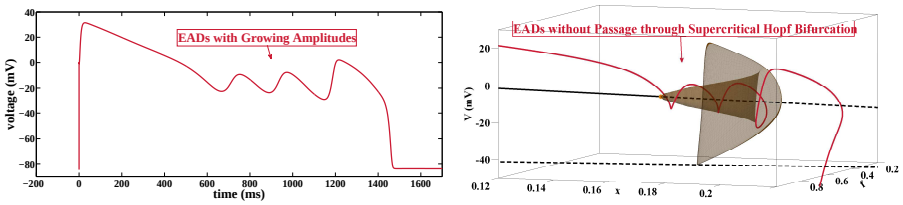

Fig. 5 Generation of EADs with growing amplitudes via direct attraction towards the stable limit cycles from outside. As opposed to the scenarios given in Figures 3 and 4, the trajectory does not pass through the supercritical Hopf point. Again, EAD termination takes place via a saddle-homoclinic bifurcation.

of attraction of the stable limit cycles. Second, Figure 5 illustrates that an actual passage through the supercritical Hopf point is not needed for the generation of EADs with growing amplitudes. In this alternative, the trajectory of the full system (1) passes by the basin of attraction of the stable focus nodes and is rather directly attracted towards the stable limit cycles from outside.

The common basis of the three cases of EAD generation with growing amplitudes discussed so far is the existence of stable limit cycles with growing amplitudes in the fast subsystem of the AP model. Our subsequent analysis reveals that at least two alternative dynamic mechanisms for the generation of EADs with growing amplitudes exist that both do not involve stable limit cycles. Such EADs on the one hand may also arise by passage through a subcritical Hopf bifurcation in the fast AP subsystem and on the other by approaching a saddle focus fixed point of the full AP system.

3 EADs with Growing Amplitudes by Passage through a Subcritical Hopf Bifurcation in the AP Fast Subsystem

In this section we consider the three-dimensional cardiac AP model

$$\begin{aligned} C\frac{dV}{dt} &= -G_{Ca}d_\infty(V)f(V-E_{Ca}) - G_K x(V-E_K), \\ \frac{df}{dt} &= \frac{f_\infty(V)-f}{\tau_f}, \\ \frac{dx}{dt} &= \frac{x_\infty(V)-x}{\tau_x}, \end{aligned} \tag{3}$$

that was first introduced in [15] for the analysis of chaotic AP dynamics. In comparison with (1) the fast variable d is replaced by its steady state $d_\infty(V)$ and the relaxation variables τ_f and τ_x are considered to be constant. Further simplifications are given by $\bar{x}(V) = 1$ and $I_0(V) = 0$.

Viewing (3) as a $(2,1)$ fast-slow system with fast variables V, f and slow

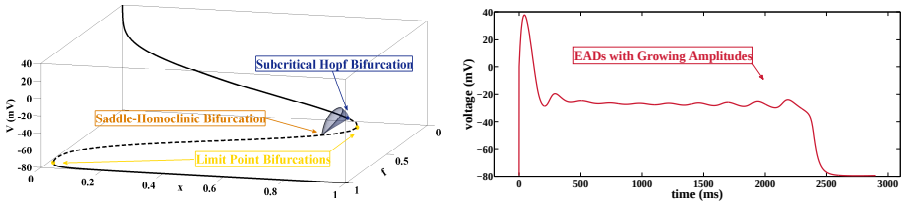

Fig. 6 **left:** Bifurcation diagram for the fast subsystem (4) with x as continuation parameter and nominal model parameters. Black solid and dashed curves represent stable and unstable fixed points of (4). At the subcritical Hopf bifurcation the stable foci turn into unstable foci. Furthermore, a branch of unstable limit cycles arises which terminates at a saddle-homoclinic bifurcation. At the limit point bifurcation the unstable focus branch collides with a branch of unstable fixed points of the saddle type. At the second limit point bifurcation, the saddle branch collides with the lower branch of stable nodes. **right:** Solution of (3) that carries EADs with growing amplitudes caused by the subcritical Hopf bifurcation.

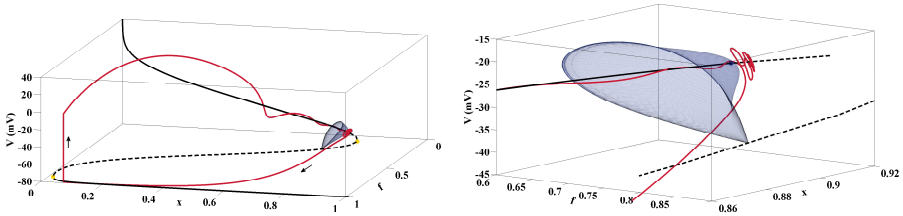

Fig. 7 Generation of EADs with growing amplitudes by passage through a subcritical Hopf bifurcation. The spiraling movement of the trajectory persists after the Hopf point for some time during which the amplitudes grow exponentially.

variable x yields the fast subsystem

$$C\frac{dV}{dt} = -G_{Ca}d_\infty(V)f(V-E_{Ca}) - G_K x(V-E_K), \qquad (4)$$
$$\frac{df}{dt} = \frac{f_\infty(V)-f}{\tau_f}.$$

A bifurcation analysis of (4) with x as continuation parameter and the model parameter values from [15] yields the bifurcation diagram displayed in Figure 6. As in the scenario displayed in Figure 2, the upper branch of stable fixed points terminates at a Hopf bifurcation, but this time the latter is of the subcritical type. In particular, the limit cycles, that emerge from the Hopf point and continue in opposite direction until their distruction at a saddle-homoclinic bifurcation, now only are unstable. Still, this bifurcation constellation admits the emergence of EADs with growing amplitudes, see Figure 6 for a corresponding solution curve of the full system (3) and Figure 7 for its projection onto the bifurcation diagram. First, the trajectory spirals around the branch of stable foci of (4). After passage through the subcritical Hopf point the trajectory again is subject to a delay effect which for some time allows the continuation of the spirals but with increasing amplitudes due to a now positive real part of the pair of complex eigenvalues. Finally, the trajectory is repelled and driven towards the lower branch of stable nodes. Note that the

saddle-homoclinic bifurcation is no longer involved in the termination of the EADs which is another significant difference to the cases discussed in Section 2.

The EAD mechanism illustrated in Figure 7 can be understood by studying the $(2,1)$-fast-slow system

$$\begin{aligned}\frac{dy_1}{dt} &= xy_1 - y_2 + y_1(y_1^2+y_2^2)^2,\\ \frac{dy_2}{dt} &= y_1 + xy_2 + y_2(y_1^2+y_2^2)^2,\\ \frac{dx}{dt} &= \varepsilon,\end{aligned} \tag{5}$$

where the fast subsystem obtained with $\varepsilon = 0$ correspond to the normal form of a subcritical Hopf bifurcation [9] at the origin $(y_1, y_2, x) = (0,0,0)$. The linearization of the fast subsystem around $(0,0)$ yields

$$\begin{aligned}\frac{d\tilde{y}_1}{dt} &= x\tilde{y}_1 - \tilde{y}_2,\\ \frac{d\tilde{y}_2}{dt} &= \tilde{y}_1 + x\tilde{y}_2,\\ \frac{dx}{dt} &= \varepsilon\end{aligned}$$

with

$$\begin{aligned}\tilde{y}_1(t) &= y_{1,0}e^{xt}\cos(t) - y_{2,0}e^{xt}\sin(t),\\ \tilde{y}_2(t) &= y_{1,0}e^{xt}\sin(t) + y_{2,0}e^{xt}\cos(t),\\ x(t) &= \varepsilon t + x_0.\end{aligned}$$

Hence, for the neighborhood with $x > 0$ the amplitudes of the oscillatory solution always grow exponentially before the trajectory of (5) is repelled from the branch of unstable fixed points. However, it depends on the initial conditions and the speed ε at which the continuation parameter x crosses the subcritical Hopf point, if those oscillations become actually visible, see Figure 8 for an illustration.

4 EADs with Growing Amplitudes by Approaching a Saddle Focus of the Full Fast-Slow System

The cardiac AP model (3) was also used in [21] to simulate the transient impact of β-adrenergic ion channel stimulators. Choosing the model parameters used in [21], one obtains an alternative bifurcation scenario for the fast subsystem (4) with x as bifurcation parameter. As illustrated in Figure 9 the upper branch of fixed points only consists of stable foci that terminate at a limit point bifurcation of (4) such that no Hopf bifurcation exists. Still, the full system (3) may admit EAD trajectories with growing amplitudes, see Figure

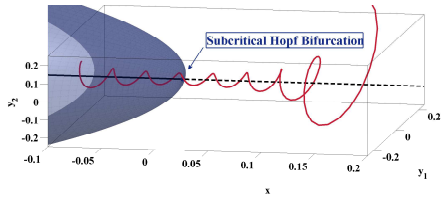

Fig. 8 Emergence of oscillations with growing amplitudes due to a delay effect associated with a subcritical Hopf bifurcation. Before the trajectory of (5) is repelled from the unstable fixed points of the fast subsystem, it spirals around them with growing amplitudes. Visibility of this effect depends on initial conditions as well as speed of passage and is given, e.g., with $(y_{1,0}, y_{2,0}, x) = (0.05, 0.05, -0.1)$ and $\varepsilon = 0.005$.

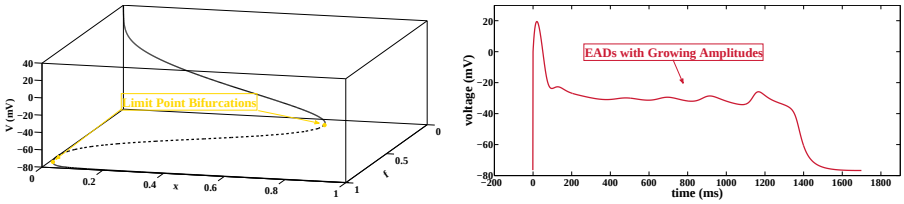

Fig. 9 **left:** Bifurcation diagram for the fast subsystem (4) with x as continuation parameter and model parameters as in [21]. Black solid and dashed curves represent stable and unstable fixed points of (4). The upper branch consists of stable foci which - as opposed to Figure 6 - only terminates at a limit point bifurcation where it turns into a branch of saddles. At the second limit point bifurcation, the saddle branch collides with the lower branch of stable nodes. **right:** Solution of (3) that carries EADs with growing amplitudes caused by a saddle focus fixed point of the full system (3).

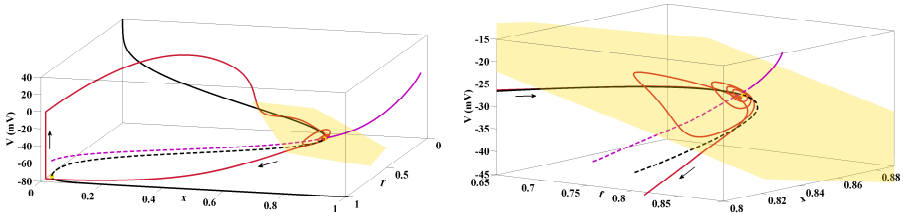

Fig. 10 Generation of EADs with growing amplitudes via a saddle focus fixed point $(\hat{V}, \hat{f}, \hat{x})$ of the full system (3) which coincides with the limit point bifurcation of the fast subsystem (4). Purple line shows branch of fixed points of (3) (with G_K as bifurcation parameter) which is crossed by the branch of fixed points of (4) at $(\hat{V}, \hat{f}, \hat{x})$. The spiraling movement of the trajectory is caused by the unstable manifold (yellow surface) spanned by the complex conjugate eigenvectors of the Jacobian at $(\hat{V}, \hat{f}, \hat{x})$.

9 for a corresponding solution curve and Figure 10 for its projection onto the bifurcation diagram. First, the trajectory spirals around the branch of stable foci of (4) and approaches the limit point bifurcation with decreasing amplitudes. The corresponding bifurcation point $(\hat{V}, \hat{f}, \hat{x})$ coincides with a saddle focus fixed point of (3) that is associated with a one-dimensional stable and a two-dimensional unstable manifold. The latter is spanned by the pair of complex conjugate eigenvectors of the Jacobian J of (3) evaluated at $(\hat{V}, \hat{f}, \hat{x})$,

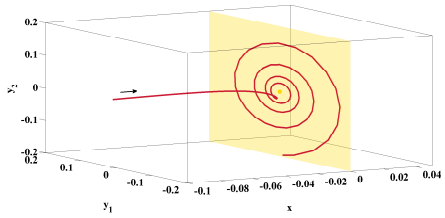

Fig. 11 Emergence of oscillations with growing amplitudes due to a saddle focus fixed point, illustrated by means of the linear system (6) with initial conditions $(y_{1,0}, y_{2,0}, x_0) = (0.01, 0.01, -0.1)$. The spiraling part of the trajectory lies on the unstable manifold (yellow surface) which is spanned by the pair of complex conjugate eigenvectors of the system matrix.

illustrated as yellow surface in Figure 10. In vicinity of $(\hat{V}, \hat{f}, \hat{x})$ the trajectory of (3) is diverted into the unstable manifold which triggers oscillations with growing amplitudes. Finally, the trajectory is repelled resulting in another turn around the stable foci of (4) before crossing the separatrix and being attracted by the lower branch of stable nodes.

The EAD mechanism illustrated in Figure 10 can be understood by studying the linear system

$$\frac{d}{dt}\begin{pmatrix} y_1 \\ y_2 \\ x \end{pmatrix} = \begin{pmatrix} 0.0026 & -0.029 & 0 \\ 0.029 & 0.0026 & 0 \\ 0 & 0 & -0.0282 \end{pmatrix} \cdot \begin{pmatrix} y_1 \\ y_2 \\ x \end{pmatrix} \tag{6}$$

which has a saddle focus at $(0, 0, 0)$. The eigenvalues of the system matrix of (6) are $\lambda_{1,2} = 0.0026 \pm 0.029 \cdot i$, $\lambda_3 = -0.0282$ and coincide with those of $J(\hat{V}, \hat{f}, \hat{x})$ for the nominal parameter setting. The stable manifold is given by the x-axis while the unstable manifold coincides with the (y_1, y_2)-plane. Figure 11 displays the behaviour of the trajectory $z(t) = e^{At} z_0$ for $z_0 = (y_{1,0}, y_{2,0}, x_0) = (0.01, 0.01, -0.1)$ and illustrates how oscillations with growing amplitudes arise on the unstable manifold of the saddle focus.

5 EADs with Decreasing Amplitudes

For the sake of completeness we mention that cardiac AP models may also produce EAD patterns with decreasing amplitudes which, however, are less observed in practice. It is argued in [21], [17] that if the Hopf-homoclinic bifurcation does not exist, the EAD oscillations (need to) dampen out. This is proven wrong by our example given in Figure 9 with growing amplitudes despite the absence of a Hopf bifurcation. Furthermore, our example given in Figure 12 shows that EAD oscillations with decreasing amplitudes may occur even in the presence of a Hopf-homoclinic bifurcation. Here, the Hopf point is basically ignored by the trajectory due to its local direction and speed such that only the branch of the stable foci with decreasing real parts of the eigenvalues has an impact. While the bifurcation properties of the fast

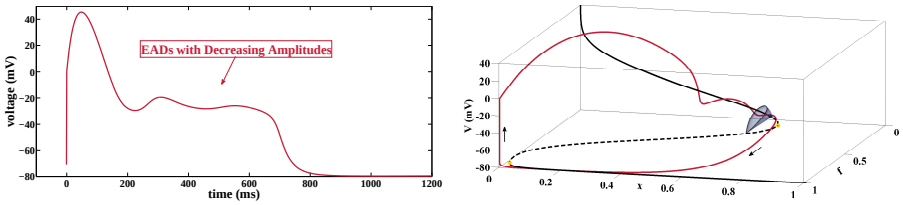

Fig. 12 EADs with decreasing amplitudes in the presence of a Hopf-homoclinic bifurcation. For EADs with growing amplitudes despite the absence of a Hopf-homoclinic bifurcation see Figure 10.

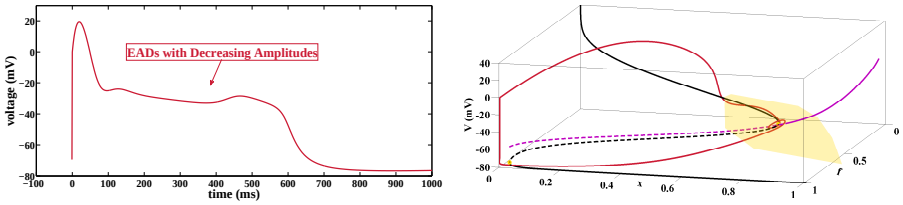

Fig. 13 EADs with decreasing amplitudes using the same fast subsystem parameters as in Figure 10 but different x-dynamics parameters. Here, the trajectory is repelled from the unstable manifold of the saddle focus only after a single turn such that an increase of amplitudes is prevented.

subsystem (4) do not depend on the dynamics of the gating variable x, the trajectory of the full system (3) of course does. It is the latter (in combination with the initial conditions of (3)) that decides if and how the trajectory is affected by the bifurcations of the fast subsystem. This is further illustrated in Figure 13 with fast subsystem model parameters identical to the ones used for Figures 9 and 10 but different parameters in the x-equation of the full system (3). As a consequence, the trajectory now only takes a single turn in the unstable manifold of the saddle focus before rejection, then resulting in an EAD pattern with decreasing amplitudes.

6 Discussion and Outlook

EADs are pathological voltage oscillations during the repolarization phase of cardiac APs. The most widely observed EAD pattern is characterized by growing amplitudes and has been previously associated [18], [14], [17] with a supercritical Hopf bifurcation in the fast subsystem of AP models. Using the parsimonious AP model (3) we in this paper have introduced two novel dynamical mechanisms for EADs with growing amplitudes, namely the passage through a subcritical Hopf bifurcation in the fast subsystem and the approach towards the unstable manifold of a saddle focus fixed point in the full AP system. As illustrated by Figure 14, the identified EAD mechanisms are not specific to the AP model used for their explanation. Random sampling of the parameter space using multivariate normal distributions (with the published parameter values taken as mean vectors) shows that both models (3) and

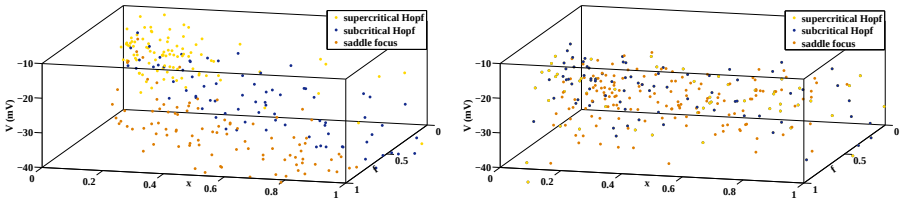

Fig. 14 The three different bifurcation scenarios (supercritical Hopf bifurcation in the fast subsystem, subcritical Hopf bifurcation in the fast subsystem and saddle focus fixed point in the full system) underlying the generation of EADs with growing amplitudes are included in the dynamic repertoire of both AP models (3) and (1). The figures display the location of the corresponding bifurcation points in the (x, f, V)-space obtained by random model parameter variation around nominal values, left for (3) and right for (1).

model (1) feature all the bifurcation scenarios outlined in the paper (supercritical Hopf bifurcation in the fast subsystem, subcritical Hopf bifurcation in the fast subsystem and saddle focus fixed point in the full system). The bifurcation analysis of the more complex state-of-the-art AP models for animal [5], human adult [12] and human induced pluripotent stem cell derived [13] is the subject of future work in which we expect to find an even richer repertoire of possible EAD mechanisms.

Given several in-silico dynamical mechanisms for EAD generation, another future challenge is to determine if and how they can be validated experimentally. One idea is to associate the frequency spectrum of recorded voltage traces that carry EAD patterns with the different periodicities of the stable and unstable oscillatory orbits of the mathematical models. If successful, this might lead to a first bifurcation theory based classification of experimentally obtained EADs.

Knowledge of the actual dynamic EAD mechanism might also serve as a basis for the development of antiarrhythmic drugs for the prevention of cardiac arrhythmias. Given an unfavourable bifurcation scenario one then needs to identify model components that both can be targeted by drugs and, if correspondingly altered, reduce or even eliminate the risk of EAD generation. One possible mathematical approach is to use inverse bifurcation analysis [1], [8] which, however, needs to be extended to, e.g., subcritical Hopf bifurcations or limit point bifurcations that coincide with saddle focus fixed points.

Finally, an understanding of the dynamic EAD mechanisms might also contribute to an improvement of preclinical drug cardiotoxicity testing. While cardiac AP models are currently used to simulate the impact of drugs on the AP trajectory [19], it might be more illuminative to directly study the drug impact on the bifurcation properties. Then, the latter may be used to define novel classifications of the proarrhythmic risk of candidate drugs.

References

1. Engl, H.W., Flamm, C., Kügler, P., Lu, J., Müller, S., Schuster, P.: Inverse problems in systems biology. Inverse Problems **25**(12), 123,014 (2009). URL http://stacks.iop.org/0266-5611/25/i=12/a=123014
2. Fermini, B., Fossa, A.A.: The impact of drug-induced qt interval prolongation on drug discovery and development. Nature reviews Drug discovery **2**(6), 439–447 (2003)
3. H. S. Karagueuzian, H. Stepanyan, and W. J. Mandel: Bifurcation theory and cardiac arrhythmias. American Journal of Cardiovascular Disease **3**(1), 1–16 (2013)
4. Hille, B.: Ion Channels of Excitable Membranes. Sinauer Associates (2001)
5. Hund, T.J., Rudy, Y.: Rate dependence and regulation of action potential and calcium transient in a canine cardiac ventricular cell model. Circulation **110**(20), 3168–3174 (2004). DOI 10.1161/01.CIR.0000147231.69595.D3
6. Krogh-Madsen, T., Christini, D.J.: Nonlinear dynamics in cardiology. Annual Review of Biomedical Engineering **14**(1), 179–203 (2012). DOI 10.1146/annurev-bioeng-071811-150106. URL http://dx.doi.org/10.1146/annurev-bioeng-071811-150106. PMID: 22524390
7. Kuehn, C.: Multiple Time Scale Dynamics, vol. 191. Springer (2015)
8. Kügler, P.: A sparse update method for solving underdetermined systems of nonlinear equations applied to the manipulation of biological signaling pathways. SIAM Journal on Applied Mathematics **72**(4), 982–1001 (2012). DOI 10.1137/110834780. URL http://dx.doi.org/10.1137/110834780
9. Kuznetsov, Y.A.: Elements of applied bifurcation theory, vol. 112. Springer Science & Business Media (2013)
10. Luo, C.H., Rudy, Y.: A model of the ventricular cardiac action potential. depolarization, repolarization, and their interaction. Circulation Research **68**(6), 1501–26 (1991). DOI 10.1161/01.RES.68.6.1501. URL http://circres.ahajournals.org/content/68/6/1501.abstract
11. Martin, C.A., Matthews, G.D.K., Huang, C.L.H.: Sudden cardiac death and inherited channelopathy: the basic electrophysiology of the myocyte and myocardium in ion channel disease. Heart **98**(7), 536–543 (2012). DOI 10.1136/heartjnl-2011-300953. URL http://heart.bmj.com/content/98/7/536.abstract
12. O'Hara, T., Virág, L., Varró, A., Rudy, Y.: Simulation of the undiseased human cardiac ventricular action potential: Model formulation and experimental validation. PLoS Comput Biol **7**(5), e1002,061 (2011). DOI 10.1371/journal.pcbi.1002061
13. Paci, M., Hyttinen, J., Aalto-Setl, K., Severi, S.: Computational models of ventricular- and atrial-like human induced pluripotent stem cell derived cardiomyocytes. Annals of Biomedical Engineering **41**(11), 2334–2348 (2013). DOI 10.1007/s10439-013-0833-3. URL http://dx.doi.org/10.1007/s10439-013-0833-3
14. Qu, Z., Xie, L.H., Olcese, R., Karagueuzian, H.S., Chen, P.S., Garfinkel, A., Weiss, J.N.: Early afterdepolarizations in cardiac myocytes: beyond reduced repolarization reserve. Cardiovascular Research **99**(1), 6–15 (2013). DOI 10.1093/cvr/cvt104
15. Sato, D., Xie, L.H., Nguyen, T.P., Weiss, J.N., Qu, Z.: Irregularly appearing early afterdepolarizations in cardiac myocytes: Random fluctuations or dynamical chaos? Biophysical Journal **99**(3), 765 – 773 (2010). DOI http://dx.doi.org/10.1016/j.bpj.2010.05.019. URL http://www.sciencedirect.com/science/article/pii/S0006349510006259
16. Sato, D., Xie, L.H., Sovari, A.A., Tran, D.X., Morita, N., Xie, F., Karagueuzian, H., Garfinkel, A., Weiss, J.N., Qu, Z.: Synchronization of chaotic early afterdepolarizations in the genesis of cardiac arrhythmias. Proceedings of the National Academy of Sciences **106**(9), 2983–2988 (2009). DOI 10.1073/pnas.0809148106. URL http://www.pnas.org/content/106/9/2983.abstract
17. Song, Z., Ko, C.Y., Nivala, M., Weiss, J.N., Qu, Z.: Calcium-voltage coupling in the genesis of early and delayed afterdepolarizations in cardiac myocytes. Biophysical Journal **108**(8), 1908 – 1921 (2015). DOI http://dx.doi.org/10.1016/j.bpj.2015.03.011. URL http://www.sciencedirect.com/science/article/pii/S0006349515002441
18. Tran, D.X., Sato, D., Yochelis, A., Weiss, J.N., Garfinkel, A., Qu, Z.: Bifurcation and chaos in a model of cardiac early afterdepolarizations. Phys. Rev. Lett. **102**(25), 258,103 (2009). DOI 10.1103/PhysRevLett.102.258103. URL http://link.aps.org/doi/10.1103/PhysRevLett.102.258103

19. Wiśniowska, B., Mendyk, A., Fijorek, K., Polak, S.: Computer-based prediction of the drug proarrhythmic effect: problems, issues, known and suspected challenges. Europace **16**(5), 724–735 (2014). DOI 10.1093/europace/euu009
20. Xie, L.H., Chen, F., Karagueuzian, H.S., Weiss, J.N.: Oxidative stress-induced afterdepolarizations and calmodulin kinase ii signaling. Circulation Research **104**(1), 79–86 (2009). DOI 10.1161/CIRCRESAHA.108.183475. URL http://circres.ahajournals.org/content/104/1/79.abstract
21. Xie, Y., Izu, L.T., Bers, D.M., Sato, D.: Arrhythmogenic transient dynamics in cardiac myocytes. Biophysical Journal **106**(6), 1391 – 1397 (2014). DOI http://dx.doi.org/10.1016/j.bpj.2013.12.050. URL http://www.sciencedirect.com/science/article/pii/S0006349514000848